JACS
JOURNAL OF THE AMERICAN CHEMICAL SOCIETY
pubs.acs.org/JACS
Article

# Direct Activation of the C($sp^3$)–$NH_2$ Bond of Primary Aliphatic Alkylamines by a High-Valent $Co^{III,IV}_2(\mu\text{-}O)_2$ Diamond Core Complex

Yan Li, Suhashini Handunneththige, Jin Xiong, Yisong Guo,* Marat R. Talipov,* and Dong Wang*

Cite This: J. Am. Chem. Soc. 2023, 145, 2690–2697

Read Online

ACCESS | Metrics & More | Article Recommendations | Supporting Information

**ABSTRACT:** Aliphatic alkylamines are abundant feedstock and versatile building blocks for many organic transformations. While remarkable progress has been made to construct C–N bonds on aliphatic and aromatic carbon centers, the activation and functionalization of C($sp^3$)–$NH_2$ bonds in primary alkylamines remain a challenging process. In the present work, we discovered an unprecedented method to directly activate the C($sp^3$)–$NH_2$ bond of primary alkylamines by a high-valent dinuclear $Co^{III,IV}_2(\mu\text{-}O)_2$ diamond core complex. This reaction results in the installation of other functional groups such as halides and alkenes onto the $\alpha$-carbon center concomitant with the 2-$e^-$ oxidation of the nitrogen atom on the amino group to form $NH_2OH$. These results shed light on future development enabling versatile functionalization of primary alkylamines based on the dinuclear cobalt system. Moreover, our work suggests that a related high-valent copper-oxo intermediate is likely generated in the ammonia monooxygenase catalytic cycle to affect the oxidation of $NH_3$ to $NH_2OH$.

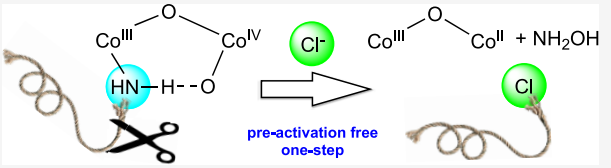




## INTRODUCTION

Aliphatic alkylamines are abundant feedstock and versatile building blocks in a variety of important biological and synthetic transformations through the construction and activation of their C–N bonds.[1] A number of redox- and non-redox-based biological processes invoke the cleavage of C–N bonds, such as ubiquitous transamination,[2,3] cross exchange of an amino group and a hydrogen atom on vicinal carbon atoms,[4] and deaminative conversion of alkylamine to aldehyde.[5,6] In particular, deaminative oxidations of primary alkylamines are typically catalyzed by amine oxidases, including the copper-containing amine oxidases (CuAOs) and the flavin-containing monoamine and polyamine oxidases (MAOs and PAOs),[5,6] to form aldehydes and ammonia: $RCH_2NH_2 + H_2O + O_2 \rightarrow RCHO + NH_3 + H_2O_2$. This reaction affords the oxidation of the $\alpha$-carbon site on the alkyl chain instead of the nitrogen atom of the amino group upon the cleavage of the C–N bond. Interestingly, in contrast, the ammonia-oxidizing enzyme ammonia monooxygenase (AMO) catalyzes the 2-$e^-$ oxidation of $NH_3$ to $NH_2OH$ with the formation of the N–O bond,[7] the first reaction of a natural nitrification process that plays key roles in global carbon and nitrogen cycling.[8] AMO is a copper-dependent enzyme and a homolog of the methane-oxidizing enzyme particulate methane monooxygenase (pMMO),[9−11] although its structure and reaction mechanism are yet to be described.

In synthetic chemistry, remarkable progress has been made to construct C–N bonds on aliphatic and aromatic carbon centers through recent developments of C–H bond amination and C–N bond cross-coupling reactions.[12−14] On the other hand, the activation of C–N bonds, particularly the unactivated C($sp^3$)–$NH_2$ bonds in primary aliphatic alkylamines, has been much less studied.[15,16] The conversion of C($sp^3$)–$NH_2$ bonds to other functionalized moieties is generally a difficult process due to their strong C–N bonds and two reactive N–H bonds. Available deaminative cross-coupling methods typically require pre-activation of the C($sp^3$)–$NH_2$ bonds to form imine, ammonium, or alkylpyridinium species (Katritzky salts, prepared by the reactions of alkylamines with the pyrylium salts) before the C–N bonds can be cleaved (Scheme 1).[15,17−25] Although direct approaches to activate C($sp^3$)–$NH_2$ bonds are available, they are limited to specific classes of alkylamines such as $\alpha$-aminoalkylferrocenes and amino acids.[26,27]

Recently, we reported the characterization and reactivity studies of a high-valent bis-$\mu$-oxo $Co^{III,IV}_2(\mu\text{-}O)_2$ diamond core complex (**1**), obtained by one-electron oxidation of the $Co^{III}_2(\mu\text{-}O)_2$ precursor (**1a**), as the synthetic mimic of the reactive diiron(IV) intermediate **Q** of soluble methane monooxygenase (sMMO).[28,29] **1** is able to cleave the $sp^3$ C–H bond up to 87 kcal/mol and is much more reactive than the diiron and dicopper analogues.[29] More importantly, the full oxidizing power of **1** can be further released upon interacting with Lewis bases to open up its diamond core and generate a terminal $Co^{IV}$–O moiety, resulting in a million-fold rate enhancement and the ability to cleave stronger C–H bonds up

Received: December 11, 2022
Published: January 23, 2023




https://doi.org/10.1021/jacs.2c13199
J. Am. Chem. Soc. 2023, 145, 2690–2697

**Scheme 1. Strategies for Activating the C(sp$^3$)−NH$_2$ Bond of Primary Aliphatic Alkylamines**

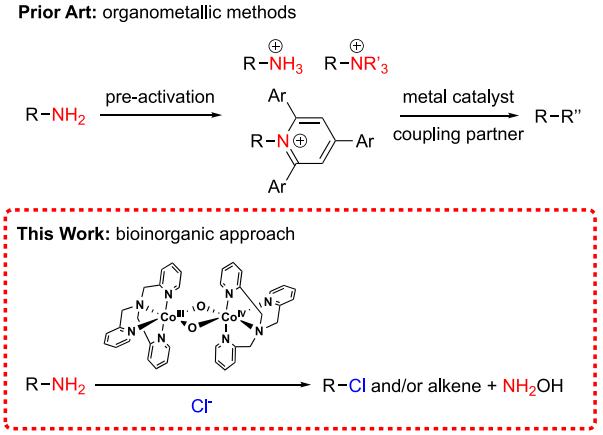


to 96 kcal/mol.[28] Specifically, when OH$^-$ is employed as the Lewis base, a *cis*-open core species HO−Co$^{III}$−O−Co$^{IV}$−O is generated based on our density functional theory (DFT) calculations, where a hydrogen bond is formed between the Co$^{III}$−OH and Co$^{IV}$−O moieties.

In this report, we discovered an unprecedented C(sp$^3$)−NH$_2$ bond activation reactivity of the diamond core complex **1** with primary aliphatic alkylamines to form alkyl chlorides and/or alkenes and hydroxylamine (Scheme 1). This deaminative reaction results in the installation of other functional groups such as chloride and C=C double bond onto the $\alpha$-carbon center concomitant with the 2-e$^-$ oxidation of the nitrogen atom on the amino group (instead of the $\alpha$-carbon center as in amine oxidases) to form a N−O bond. The formation of alkyl chloride and alkene is strongly affected by the structural and electronic properties of the alkylamine substrates, an approach that can be employed to predict the reaction outcomes. Our work has thus provided an unprecedented method to directly activate and functionalize the C(sp$^3$)−NH$_2$ bond of primary aliphatic alkylamines, a new organic transformation that has yet to be reported in previous discoveries. On the other hand, the oxidation of the amino group/ammonia to hydroxylamine by the high-valent dicobalt species is a synthetic mimic for the enzymatic reaction of AMO, which suggests that a related high-valent copper-oxo species is likely generated as the key intermediate to carry out the ammonia oxidation and N−O bond formation in the enzymatic catalytic cycle.

## RESULTS AND DISCUSSION

We first selected 4-phenylbutylamine (PBA, **2**, p$K_a$ = 10.21 in aqueous solution) as a probe substrate to investigate the reaction of **1** with alkylamines, with the original goal of evaluating any possible site-selective C−H bond oxidation on the alkyl chain. The introduction of only 1 equiv of PBA into the methanol solution of **1** at −60 °C causes the increase in the self-decay rate of **1** by 1 order of magnitude from 0.008 to 0.076 s$^{-1}$. This rate is about 3-fold faster than those observed for **1** in the presence of other simple Lewis bases reported in our previous work.[28] The reaction follows first-order kinetics (Figure S1) without the formation of any other intermediate. Surprisingly, this dicobalt-PBA adduct is unable to react with external substrates such as toluene. As shown in Figure 1A, the addition of large excess amounts of toluene does not result in any enhancement of the rate constant, indicating that

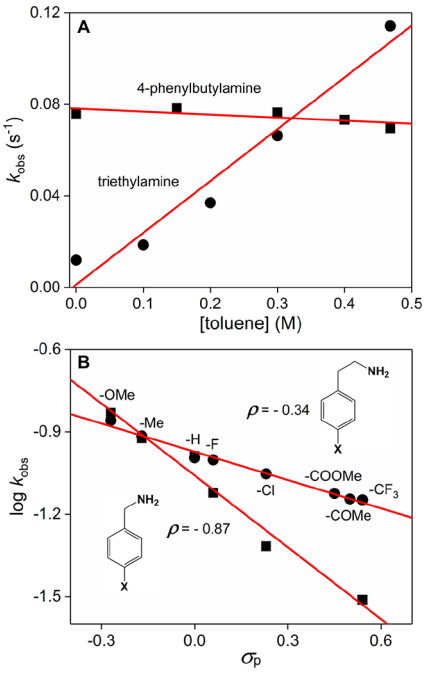


**Figure 1.** (A) Plots of $k_{obs}$ as a function of the substrate concentration for toluene oxidation by 0.15 mM **1** in the presence of 1 equiv of 4-phenylbutylamine (square) and triethylamine (circle), obtained in MeOH at −60 °C. The lines represent the best linear fittings. (B) Hammett correlations for the reaction of **1** with *para*-X-substituted benzylamine (square) and phenethylamine (circle) derivatives.

intermolecular C−H bond oxidations by **1**, as we previously observed,[28,29] are completely inhibited by the presence of only 1 equiv of PBA. In contrast, a typical second-order rate constant ($k_2$) of 0.23(3) M$^{-1}$ s$^{-1}$ is measured for toluene oxidation by **1** in the presence of 1 equiv of triethylamine (p$K_a$ = 10.8). These results clearly indicate that primary and tertiary alkylamines have distinct effects on the reactivity of the diamond core complex **1**.

Analysis of the reaction products of PBA by GC−MS showed the formation of 1-chloro-4-phenylbutane (12% yield) and 4-phenyl-1-butene (36% yield, all yields are referred to **1**), accounting for ∼50% of the oxidizing equivalents used (Figure S2). The formation of ketone and aldehyde products is not detected even if the reaction is carried out in air. Together, these observations suggest that (a) there is an intramolecular reaction pathway of the dicobalt-PBA adduct that outcompetes the intermolecular C−H bond cleavage of toluene, and (b) this intramolecular reaction affords the deamination of the alkyl chain to form the chlorinated and desaturated products, both of which require the activation of the C−NH$_2$ bond presumably in a heterolytic manner. The lack of ketone and aldehyde products in the presence of O$_2$ is strong evidence against the formation of a carbon radical as the result of homolytic C−NH$_2$ bond cleavage. We carried out careful control experiments to exclude any background oxidation of PBA by residual CAN in the solution (see the Supporting Information for more information). We also measured the oxidation potentials of both PBA and CAN using cyclic voltammetry, showing that CAN is unable to oxidize PBA under our experimental conditions (Figure S3).

The source of chloride appears to be the starting Co(II) complex Co(II)(TPA)Cl$_2$. Only the desaturated but not the chlorinated product was observed if the perchlorate form


https://doi.org/10.1021/jacs.2c13199
J. Am. Chem. Soc. 2023, 145, 2690−2697

**Table 1. Substrate Scope of C($sp^3$)–$NH_2$ Bond Activation Reactions by 1 in Methanol at −60 °C with 30 equiv of TBACl (Optimized Condition for Alkyl Chloride Formation)**[a]

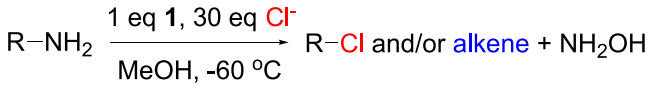


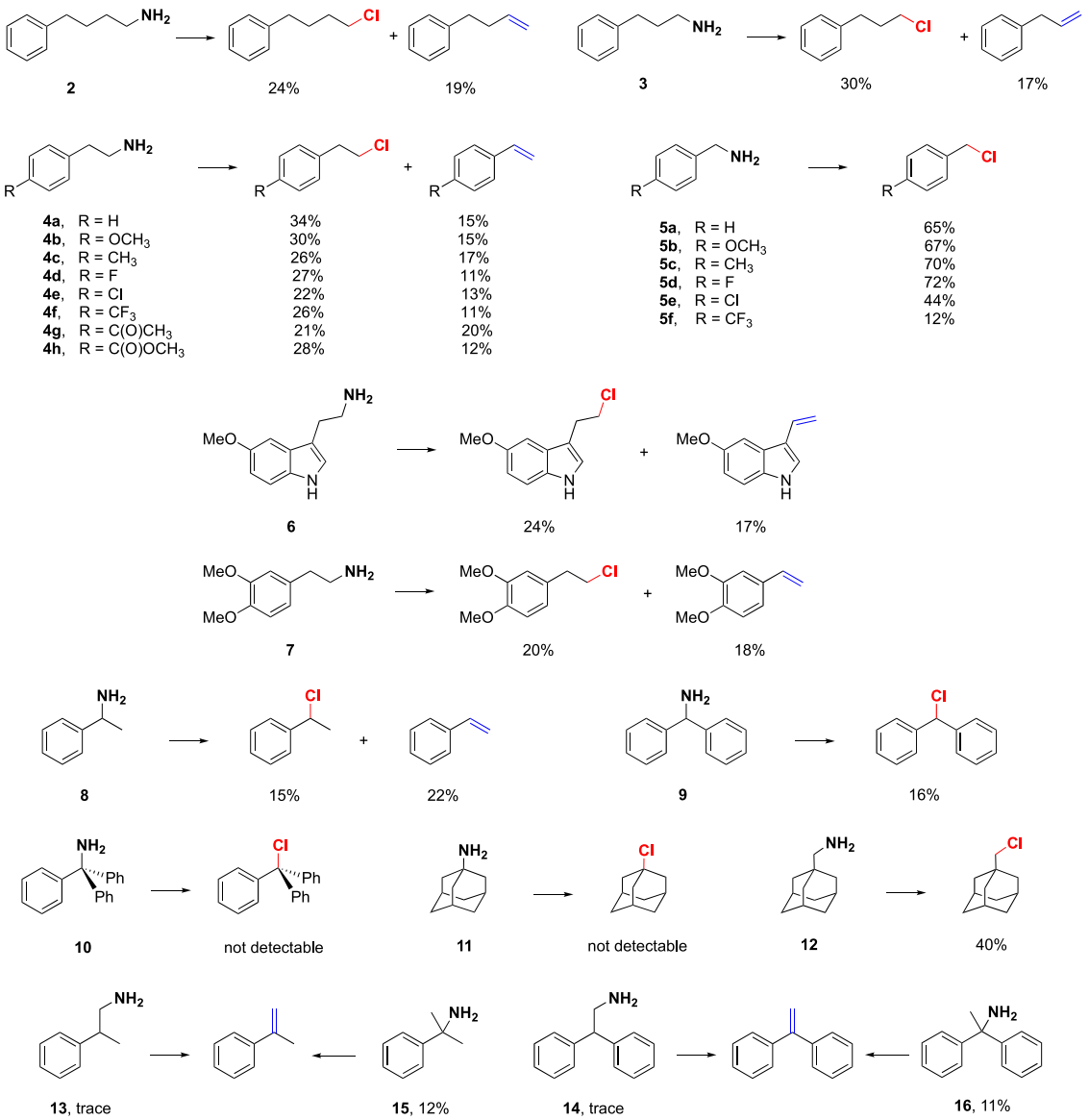


[a]All product yields are determined by GC–MS and normalized to the formation yield of complex **1**. See the Supporting Information for more details.

$Co(II)(TPA)(ClO_4)_2$ is used as the starting complex for the same experiment (Figure S4). We then optimized experimental conditions for the formation of 1-chloro-4-phenylbutane using tetrabutylammonium chloride (TBACl) as the $Cl^-$ source and found that its highest yield (24%) can be obtained with a ratio of **1**:PBA:$Cl^-$ = 1:1:30 at a $Cl^-$ concentration of ∼0.1 M (Figure S5A and Tables S1 and S2). The addition of too much chloride above the optimized ratio inhibits the formation of both the alkyl chloride and alkene, presumably because the direct reaction of $Cl^-$ with the dicobalt-PBA adduct becomes significant at high $Cl^-$ concentrations. On the other hand, increasing the amount of PBA increases the formation of the alkene (up to 32% yield) but decreases the yield of the alkyl chloride (Figure S5B). We hypothesize that this is because the excess amount of PBA acts as a Lewis base to promote the deprotonation necessary to form the alkene (see more details in later discussions). On the other hand, when $Cl^-$ is replaced by $Br^-$ in the solution, we observed the formation of 1-bromo-4-phenylbutane in a yield (26%) similar to that of 1-chloro-4-phenylbutane (Figure S6). Furthermore, no halogenation product was identified if $F^-$ or $I^-$ is used as the nucleophile.

We expanded the substrate scope (Table 1) to investigate the effects of the steric and electronic properties of the alkylamines on their reactions with **1** under the optimized conditions for the alkyl chloride formation (30 equiv of $Cl^-$). For each amine substrate studied, we measured the rate


https://doi.org/10.1021/jacs.2c13199
J. Am. Chem. Soc. 2023, 145, 2690−2697

constant and quantified the reaction product(s) (Table S1). For amines that afford low product yields (such as **5f**, **9**, **15**, and **16**), we typically recovered >50% of the starting substrates. Our results show that, for alkylamines (**2**−**4a**) that have a linear alkyl chain between a phenyl ring and the terminal amino group and are able to form both the alkyl chloride and alkene, the reaction appears to favor slightly the formation of alkyl chloride as the alkyl chain becomes shorter, while the typical combined product formation yields are 40−50% (Figures S7−S9). For benzylamine (**5a**), the simplest substrate in this category where it is impossible to form the alkene product, we observed the formation of benzyl chloride in 65% yield.

The overall C−$NH_2$ bond cleavage is strongly affected by the electronic properties of the amine substrates. We employed benzylamine and its derivatives with a variety of *para*-substituents as a set of test substrates (**5a**-**f**) and found that the substrates with electron-donating groups (EDG) react faster with **1** and afford the corresponding alkyl chlorides in higher yields compared to those with electron-withdrawing groups (EWG) (Figures S10−S22). The Hammett plot (Figure 1B) clearly shows that the logarithm of the reaction rate constant $k_{obs}$ correlates linearly as a function of the Hammett parameter $\sigma_{para}$ of the aromatic substituents with a slope of $\rho = -0.87$. The negative $\rho$ value is a clear indication that the reaction builds partial positive charges on the benzylic carbon center. Interestingly, the Hammett plot of phenethylamine and derivatives (**4a**-**h**), where a $CH_2$ spacer is placed between the benzylic carbon site and the amino group, affords also a linear correlation but with a much smaller slope of $\rho = -0.34$ (Figure 1B). This result indicates that the *para*-substituents on the phenyl ring have a reduced effect on the $\alpha$-carbon center as the alkyl chain becomes longer. This group of substrates (**4a**-**h**) affords both the alkyl chloride and alkene in typical yields of 20−35 and 10−20%, respectively (Figures S23−S36). Notably, substrates derived from two bioactive alkaloids, including serotonin and dopamine derivatives having related arylethylamino moieties (5-methoxytryptamine, **6**, and 3,4-dimethoxy-phenethylamine, **7**), are converted to the corresponding alkyl chloride and alkene in moderate yields (Figures S37−S39). These results demonstrate that our reaction is well tolerated to a broad range of functional groups at a remote position, including aryl and alkyl halides, ether, ester, ketone, and an unprotected indole ring.

For all the substrates studied, the formation of the alkyl chloride occurs only on the $\alpha$-carbon site adjacent to the amino group. No other *regio*-isomers are observed. The chlorination appears to be highly sensitive to the crowdedness of the $\alpha$-carbon center. For example, comparison of the results obtained from phenethylamine (**4a**) and $\alpha$-methylbenzylamine (**8**) shows that the formation of (2-chloroethyl)benzene (34%) is in a higher yield than (1-chloroethyl)benzene (15%; Table 1 and Figure S40), consistent with that the $\alpha$-carbon site in phenethylamine is less sterically hindered than that in $\alpha$-methylbenzylamine. Furthermore, increasing the steric hindrance of benzylamine by adding one and two phenyl rings onto the $\alpha$-carbon center (benzhydrylamine, **9**, and triphenylmethylamine, **10**) results in decreased reaction rates (Table S1) and significantly reduced alkyl chloride formation yields for this series of substrates (Table 1 and Figure S41). Specifically, the formation of the alkyl chloride is undetectable for triphenylmethylamine. Similar results (no alkyl chloride formation) are obtained also for sterically hindered substrates such as 1-adamantylamine (**11**), cumylamine (**15**), and 1,1-diphenylethan-1-amine (**16**), where the amino group is adjacent to a tertiary $\alpha$-carbon center, indicating that these $\alpha$-carbon sites are inaccessible by $Cl^-$. Interestingly, moving the steric crowdedness slightly away from the $\alpha$-carbon center of 1-adamantylamine by adding a $CH_2$ spacer between the adamantyl and the amino groups (1-adamantanemethylamine, **12**) restored the chlorination reactivity with the formation of 1-adamantanemethyl chloride in 40% yield (Figure S42). Taken together, these results clearly indicate that the chlorination occurs through an $S_N2$ nucleophilic attack of the $\alpha$-carbon center of the amine substrate by $Cl^-$ in the solution.

On the other hand, the formation of alkene appears to follow an E2 pathway, where the alkylamine also functions as a Lewis base to deprotonate the $\beta$-carbon (if applicable) and form a C=C bond in the same transition state as the C−$NH_2$ bond cleavage. We employed phenethylamine deuterated at the $\beta$-carbon site to probe this mechanism. A competition experiment with 1:1 mixed non-deuterated and deuterated phenethylamine as the substrate afforded both non-deuterated and deuterated styrene products in a ratio of ∼20:1, indicating an H/D kinetic isotope effect (KIE) of ∼20. This large KIE strongly suggests that the cleavage of the $\beta$-C−H bond is a significant component of the rate-determining step. In addition, substrates with a tertiary $\alpha$- or $\beta$-carbon site afforded alkenes with much reduced yields. For example, only trace amounts of alkene products are observed for $\beta$-methylphenethylamine (**13**) and 2,2-diphenylethylamine (**14**), likely due to the steric inaccessibility of their $\beta$-protons by the Lewis base in the course of the reactions. Furthermore, cumylamine (**15**) and 1,1-diphenylethylamine (**16**) (*regio*-isomers of **13** and **14**, respectively) afforded the formation of alkenes in only ∼10% yields (Figures S43 and S44), much lower than those substrates with $\alpha$-CH−$NH_2$ or $\alpha$-$CH_2$−$NH_2$ moieties. The steric hindrance of the $\alpha$-carbon site in these two alkylamines likely makes it difficult for them to access the substrate $\beta$-protons in an E2 reaction as a Lewis base. Notably, these sterically hindered alkylamines (**10**, **11**, **15**, and **16**) all react with **1** in a rate that is typically 3- to 5-fold slower than those of other alkylamine substrates (Table S1), indicating that these subsets of substrates have weaker binding abilities to the cobalt center due to the sterically hindered $\alpha$-carbon center. This E2 process is also consistent with our observations that the alkene formation yield is dependent on the amine concentration in the reaction solutions (Figures S5 and S45), and substrates **2** and **3** afford the corresponding alkenes with the C=C bond at the terminal position of the alkyl chain without the formation of other *regio*-isomers, which otherwise is expected for an E1 process.

The lack of formation of the ketone or aldehyde product in our reactions strongly indicates that the alkyl chain is not oxidized. Therefore, we hypothesize that the amino group is oxidized by the high-valent dicobalt species to generate a 2-$e^-$ oxidized species, likely $NH_2OH$. Indeed, product analysis of the post-reaction solution of **1** with a representative alkylamine substrate (such as benzylamine) by ESI-MS showed the formation of a mono-cationic species with $m/z = 34$, which is assignable to $[NH_3OH]^+$. This signal shifted by one mass unit to $m/z = 35$ if $^{15}N$ enriched substrates are employed (Figure S46). Quantification of the $NH_2OH$ formation yield is carried out using $^{15}N$ NMR spectroscopy. As shown in Figure S47, the $^{15}N$ NMR spectrum of the reaction solution of **1** with $^{15}N$-labeled benzylamine (chemical shift ∼29 ppm, $^{15}N$-ammonia


https://doi.org/10.1021/jacs.2c13199
J. Am. Chem. Soc. 2023, 145, 2690−2697

as the reference) affords a signal at ∼107 ppm. Addition of a known amount of the authentic $^{15}NH_2OH$ sample into the reaction solution causes the increase in the 107 ppm signal, indicating that this signal originates from $^{15}NH_2OH$ formed from the reaction of **1** with benzylamine (see the Supporting Information for more details). Integrations of the 107 ppm signal further showed that $NH_2OH$ is formed in a yield of ∼60%, consistent with a formation yield of 65% for benzyl chloride obtained by GC−MS. Moreover, to further verify that complex **1** is able to oxidize the nitrogen atom of an amino group without an alkyl chain, we employed $^{15}N$-ammonia as the substrate to react with **1**. As shown in Figure S48, the $^{15}N$ NMR spectrum of the reaction solution clearly shows the formation of $^{15}NH_2OH$ as the only product in ∼60% yield. Therefore, our reaction mimics the one catalyzed by the enzyme AMO.

We carried out electron paramagnetic resonance (EPR) studies to further examine the fate of the dicobalt complex in the aforementioned reactions. The starting $Co^{III}{}_2(\mu\text{-}O)_2$ complex **1a** is diamagnetic and EPR silent (Figure 2A). The

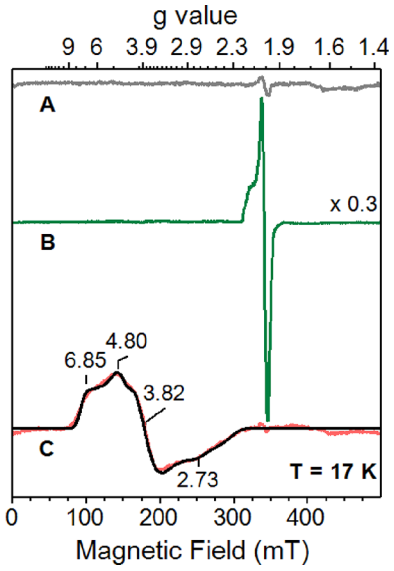


**Figure 2.** X-band EPR spectra of **1a**, **1**, and **1b**. (A) **1a**; (B) sample containing **1** obtained by treating **1a** with CAN; (C) sample containing **1b** by treating 1 mM **1a** with 3 mM CAN and then treating it with 0.2 M $NH_3$. The black line shows the corresponding simulation for **1b**. The simulation parameters are $g$ = [2.50, 2.38, 2.87], $A(^{59}Co)$ = [100, 240, 390] MHz, $D$ = +50 $cm^{-1}$, $E/D$ = 0.15, and $\sigma(E/D)$ = 0.04. The data collection conditions are a microwave frequency of 9.63 GHz, microwave power of 2 mW, modulation frequency of 100 KHz, modulation amplitude of 0.5 mT, and temperature of 17 K. See the Supporting Information for discussion on the simulation.

oxidation of **1a** by CAN afforded the mixed-valent $Co^{III,IV}{}_2(\mu\text{-}O)_2$ complex **1** as an $S$ = 1/2 species with an EPR signal centered at $g$ ∼2 (Figure 2B). Spin quantification of this signal suggests that the formation yield of complex **1** is ∼60 to 70%. These results are consistent with the ones that we reported previously for **1**.[29] The addition of $NH_3$ to the solution of **1** resulted in the complete decay of the $S$ = 1/2 species and the concomitant formation of a new, broad EPR signal with observed $g$ resonances at 6.85, 4.80, 3.82, and 2.73 (Figure 2C), which is assignable to an $S$ = 3/2 Co(II) species (**1b**). The observed EPR signal originates from the $M_S$ = ±1/2 Kramers doublet of an $S$ = 3/2 spin state. The temperature-dependent EPR measurements suggested that this $M_S$ = ±1/2 Kramers doublet should be the ground doublet (Figure S49); thus, the axial zero field splitting ($D$) of **1b** should be positive. The simulation and quantification of this signal (see Figure 2 and the figure caption) indicated that the formation yield of **1b** is 80 ± 20% (average of six samples, see Table S3 for more details) from complex **1**, suggesting that **1** is a 2-$e^-$ oxidant in the course of reaction with $NH_3$. Given the basic reaction environment with added amine/ammonia, we propose that **1b** is mixed-valent dicobalt(II,III) species.

**Mechanistic Considerations.** We propose a mechanistic sketch (Scheme 2) that highlights the key fundamental steps

**Scheme 2. Schematic Illustration for the Reaction Pathway of 1 with PBA**

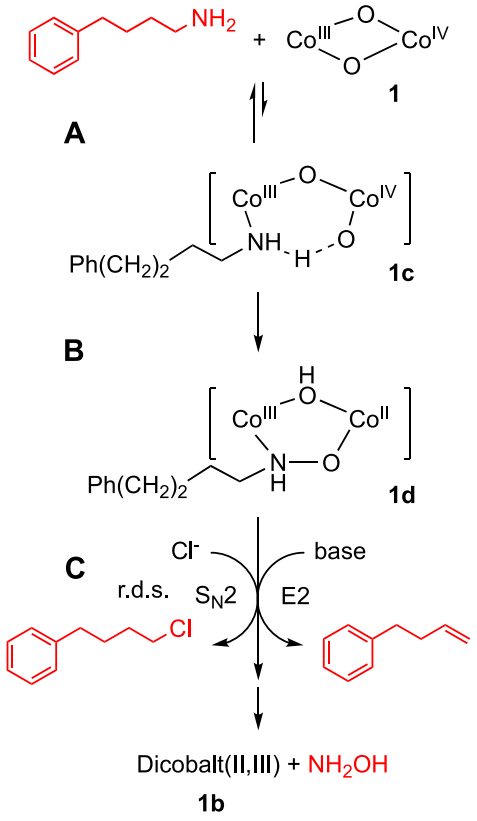


necessary for this novel transformation. Detailed computational investigation of the reaction mechanism is underway and will be the subject of another publication. Coordination of the alkylamine (Scheme 2, step A, using PBA as an illustrative example) first opens up the diamond core of **1** to generate an open core species **1c**. As we have demonstrated in a previous publication,[28] the binding of a Lewis base ($pK_a$ in a range of 4−16) to **1** is weak ($K_{eq}$ = 0.31 $M^{-1}$) and the equilibrium strongly disfavors the formation of the open core. Therefore, **1c** should be a minor species in the reaction solution. Given that the amino group (−$NH_2$) is also a hydrogen bond donor similar to hydroxide, we hypothesize that **1c** is a *cis*-open core adduct (instead of *trans*-open core) with a hydrogen bound N−H···O−Co(IV) moiety. We turned to DFT calculations to obtain a geometry-optimized structure of this key intermediate to better understand it. As shown in Figure 3A, ethylamine-coordinated dicobalt complex *cis*-Et$NH_2$-$Co^{III}$−O−$Co^{IV}$−O


https://doi.org/10.1021/jacs.2c13199
J. Am. Chem. Soc. 2023, 145, 2690−2697

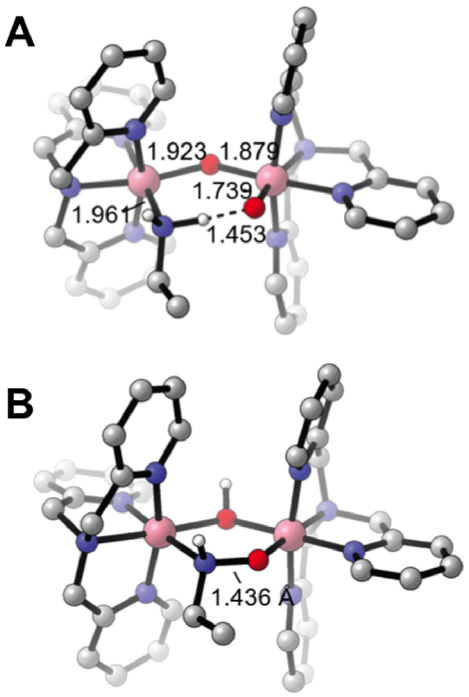


**Figure 3.** Geometry optimized structures of (A) **1c** and (B) **1d** obtained at the BP86/6-31G(D) + PCM(methanol) level of theory. Cobalt, pink; oxygen, red; nitrogen, blue; carbon, gray; hydrogen, white.

has a long Co···Co distance of 3.5 Å, characteristic of an open core configuration. Interestingly, the NH···O interatomic distance between the N−H bond and O−Co(IV) moiety of this complex is as short as 1.45 Å, which, together with a linear arrangement of the N−H···O atoms, suggests a strong intramolecular hydrogen bonding. The unpaired electron in *cis*-Et$NH_2$-$Co^{III}$−O−$Co^{IV}$−O is primarily localized on the terminal oxygen atom (+0.38 a.u.) and Co(IV) (+0.48 a.u.), exhibiting a significant radical character on the terminal oxygen atom. By contrast, tertiary alkylamines such as triethylamine are unable to form the hydrogen bound *cis*-open core configuration but rather generate a *trans*-open core upon coordinating to the cobalt center. This structural difference appears to have a significant impact on the reaction outcomes—intramolecular C−N bond cleavage with PBA vs intermolecular C−H bond activation in the presence of triethylamine (Figure 1A).

The *cis*-open core species **1c** then likely undergoes a non-rate-determining step (Scheme 2, step B) to oxidize the amino nitrogen forming a N−O bond and consume the Co(IV)−O oxidant. This hypothesis is consistent with our observations that (i) external substrates such as toluene are unable to intercept the Co(IV)−O oxidant, and (ii) weak C−H bonds in the alkylamine substrates such as the benzylic C−H bonds in benzylamine are not oxidized. We propose that this transformation affords a two-electron reduced dicobalt(II,III) species **1d**. The geometry-optimized structure of **1d** by DFT (Figure 3B) shows that it is bridged by a hydroxyl ligand and a NH−O moiety, forming a five-member ring with a N−O bond length of 1.436 Å. This structure is in accordance with a number of Co($\mu$-OH)($\mu$-OO)Co complexes reported in literature.[30−32] Our calculations show that **1d** is ∼2.4 kcal/mol more stable than **1c**, suggesting that the conversion of **1c** to **1d** is thermodynamically favorable. The formation of a N−O bond can be accomplished by the Co(IV)−O moiety in **1c** via a direct oxygen atom transfer (OAT) or following classical hydrogen atom transfer (HAT) and radical rebound processes. We favor the OAT pathway because the N−H bonds of primary alkylamines are typically strong (>100 kcal/mol), and the upper limit of the C−H bond that the Co(IV)−O oxidant can cleave is only 96 kcal/mol.[28] Although recent work from other groups has shown that the coordination of $NH_3$ to a transition metal center induces weakening of the N−H bond, the degree of perturbation is expected to be small for cobalt.[33,34]

The rate-determining step (Scheme 2, step C) appears to be the C−N bond cleavage, as clearly demonstrated by the Hammett relationship. This is a non-redox step that affords the formation of organic product(s) via the $S_N2$ or E2 pathway discussed above. We further employed $CH_3NH_2$ and $CD_3ND_2$ as probe substrates and measured their rate constants with **1**. As shown in Figure S50, these measurements afforded an H/D kinetic isotope effect (KIE) of 1.37. This value is much smaller than those observed in our previous work for C−H/C−D bond activation by the open core complex,[28] suggesting that it is not a primary KIE. Instead, we assign it to an $\alpha$-secondary KIE, consistent with the change of the $\alpha$-carbon hybridization from $sp^3$ to $sp^2$ in the $S_N2$ transition state.[35]

Furthermore, the C−N bond cleavage (step C) cannot precede the N−O bond formation (step B). Our control experiments show that no benzyl chloride is formed if benzylamine is added to a mononuclear Co(III)-TPA complex under otherwise identical conditions, indicating that the binding of the alkylamine to the cobalt center alone is insufficient to trigger C−N bond cleavage. In addition, no reaction was observed when acetamide ($CH_3C(O)NH_2$) and benzamide ($PhC(O)NH_2$) are employed as substrates, likely because the formation of the N−O bond for these two substrates is difficult due to the electron-withdrawing carbonyl group adjacent to $NH_2$, even though their $\alpha$-carbon is more electrophilic and susceptible for nucleophilic attack.

The diamond core complex **1** thus represents the first example of a high-valent metal-oxo complex that mediates direct activation of the C($sp^3$)−$NH_2$ bond of aliphatic primary alkylamines. This reaction takes advantages of the unique features of the dicobalt-alkylamine adduct, where the alkylamine is both a strong Lewis base to open the $Co^{III,IV}_2(\mu\text{-}O)_2$ diamond core and a hydrogen bond donor to "lock" the *cis*-open core configuration between the $Co^{III}$−$NH_2$ and $Co^{IV}$−O moieties. Both the open core structure and the *cis*-configuration are critical to ensure successful intramolecular C($sp^3$)−$NH_2$ bond cleavage and N−O bond formation. By contrast, the diamond core itself is unable to activate the C($sp^3$)−$NH_2$ bond. For example, a closely related $Cu^{III}_2(\mu\text{-}O)_2$ species reported recently oxidizes primary alkylamines to nitriles, a desaturation reactivity instead of heterolytic cleavage of the $RCH_2$−$NH_2$ bond.[36] The formation of the C−Cl (or C−Br) bond, on the other hand, is the result of $Cl^-$ (or $Br^-$) being both a weak Lewis base incapable of competing with the alkylamine for binding the cobalt center and a strong nucleophile in methanol for attacking the $\alpha$-carbon site. The employment of such a protic solvent further decreases the nucleophilicity (not basicity) of the primary alkylamine substrates so that no formation of secondary alkylamine is observed as the reaction product under optimized chlorination conditions.


https://doi.org/10.1021/jacs.2c13199
J. Am. Chem. Soc. 2023, 145, 2690−2697

## CONCLUSIONS

In conclusion, we have discovered a novel organic transformation that converts primary aliphatic alkylamines to functionalized product(s) via direct activation of the inert $C(sp^3)-NH_2$ bond by a high-valent $Co^{III,IV}_2(\mu\text{-}O)_2$ complex. The merits of our work are multi-fold. First, the direct method for converting aliphatic primary alkylamines to other functionalities such as alkyl halides and alkenes without any pre-activation of the $C(sp^3)-NH_2$ bond is unprecedented. Furthermore, our mechanistic studies have shown that the formation of C−Cl and C═C bonds proceeds through two separate pathways ($S_N2$ and E2, respectively), each of which can be modulated by the structural and electronic properties of the alkylamine substrates as well as the amount of $Cl^-$/amine added into the reaction solution. These conditions can thus be employed to predict the reaction outcomes and enable more complex experimental designs. At the current stage, this prototype reaction is stoichiometric and fundamental in nature. However, we envision that, in the future development of this work, nucleophiles other than $Cl^-/Br^-$ can be employed to design other C−X (X = N, O, and C) bond coupling reactions and catalytic systems can be further developed using primary alkylamines as the substrates to enable novel synthetic utilities.

On the other hand, the formation of $NH_2OH$ as the oxidation product of alkylamines/ammonia is a synthetic mimic of the enzymatic 2-$e^-$ oxidation of ammonia by AMO. Our work thus suggests that a high-valent copper-oxo intermediate is likely generated in the AMO catalytic cycle as the key oxidant. While a related enzymatic intermediate has yet to be characterized, our work has demonstrated the powerful abilities of synthetic model complexes to provide insights about enzymatic reactions.

## ASSOCIATED CONTENT

### Supporting Information

The Supporting Information is available free of charge at https://pubs.acs.org/doi/10.1021/jacs.2c13199.

Materials and methods; additional experimental details, including synthetic procedures, kinetic measurements and plots, product analysis results by GC−MS, ESI-MS, and $^1H$, $^{19}F$, and $^{15}N$ NMR spectroscopy, EPR data collection and analysis, and DFT calculations and Cartesian coordinates; and references (PDF)

## AUTHOR INFORMATION


### Corresponding Authors

**Yisong Guo** − *Department of Chemistry, Carnegie Mellon University, Pittsburgh, Pennsylvania 15213, United States;* orcid.org/0000-0002-4132-3565; Email: ysguo@andrew.cmu.edu

**Marat R. Talipov** − *Department of Chemistry and Biochemistry, New Mexico State University, Las Cruces, New Mexico 88003, United States;* orcid.org/0000-0002-7559-9666; Email: talipovm@nmsu.edu

**Dong Wang** − *Department of Chemistry and Biochemistry, Center for Biomolecular Structure and Dynamics, University of Montana, Missoula, Montana 59812, United States;* orcid.org/0000-0002-6370-1942; Email: dong1.wang@umontana.edu

### Authors

**Yan Li** − *Department of Chemistry and Biochemistry, Center for Biomolecular Structure and Dynamics, University of Montana, Missoula, Montana 59812, United States;* orcid.org/0000-0002-2623-0475

**Suhashini Handunneththige** − *Department of Chemistry and Biochemistry, New Mexico State University, Las Cruces, New Mexico 88003, United States;* orcid.org/0000-0001-5257-8013

**Jin Xiong** − *Department of Chemistry, Carnegie Mellon University, Pittsburgh, Pennsylvania 15213, United States;* orcid.org/0000-0001-7443-0554

Complete contact information is available at: https://pubs.acs.org/10.1021/jacs.2c13199


### Notes

The authors declare no competing financial interest.

## ACKNOWLEDGMENTS

Support of this work for Y.L. and D.W. was provided by the University of Montana, Montana INBRE (IDeA Networks of Biomedical Research Excellence, grant NIGMS P20GM103474) and National Science Foundation (grant CHE-2102339). S.H. and M.R.T. were supported by an Institutional Development Award (IDeA) from the National Institute of General Medical Sciences (grant P20GM103451). The DFT calculations were performed using computational resources awarded by the Extreme Science and Engineering Discovery Environment (XSEDE) TG-CHE170004. J.X. and Y.G. thank the support from NIGMS grants P01GM125924 and P01GM127588.

## REFERENCES


(1) Froidevaux, V.; Negrell, C.; Caillol, S.; Pascault, J.-P.; Boutevin, B. Biobased Amines: From Synthesis to Polymers Present and Future. *Chem. Rev.* **2016**, *116*, 14181−14224.

(2) Cai, W.; Qiao, X.; Zhang, H.; Li, B.; Guo, J.; Zhang, L.; Chen, W.-W.; Zhao, B. Asymmetric Biomimetic Transamination of α-keto Amides to Peptides. *Nat. Commun.* **2021**, *12*, 5174.

(3) Mayer, R. J.; Kaur, H.; Rauscher, S. A.; Moran, J. Mechanistic Insight into Metal Ion-Catalyzed Transamination. *J. Am. Chem. Soc.* **2021**, *143*, 19099−19111.

(4) Wu, B.; Szymański, W.; Heberling, M. M.; Feringa, B. L.; Janssen, D. B. Aminomutases: Mechanistic Diversity, Biotechnological Applications and Future Perspectives. *Trends Biotechnol.* **2011**, *29*, 352−362.

(5) Klema, V. J.; Wilmot, C. M. The Role of Protein Crystallography in Defining the Mechanisms of Biogenesis and Catalysis in Copper Amine Oxidase. *Int. J. Mol. Sci.* **2012**, *13*, 5375−5405.

(6) Cona, A.; Rea, G.; Angelini, R.; Federico, R.; Tavladoraki, P. Functions of Amine Oxidases in Plant Development and Defence. *Trends Plant Sci.* **2006**, *11*, 80−88.

(7) Norton, J. M.; Alzerreca, J. J.; Suwa, Y.; Klotz, M. G. Diversity of Ammonia Monooxygenase Operon in Autotrophic Ammonia-oxidizing Bacteria. *Arch. Microbiol.* **2002**, *177*, 139−149.

(8) Heil, J.; Vereecken, H.; Brüggemann, N. A Review of Chemical Reactions of Nitrification Intermediates and Their Role in Nitrogen Cycling and Nitrogen Trace Gas Formation in Soil. *Eur. J. Soil Sci.* **2016**, *67*, 23−39.

(9) Fisher, O. S.; Kenney, G. E.; Ross, M. O.; Ro, S. Y.; Lemma, B. E.; Batelu, S.; Thomas, P. M.; Sosnowski, V. C.; DeHart, C. J.; Kelleher, N. L.; Stemmler, T. L.; Hoffman, B. M.; Rosenzweig, A. C. Characterization of a Long Overlooked Copper Protein from Methane- and Ammonia-oxidizing Bacteria. *Nat. Commun.* **2018**, *9*, 4276.

(10) Musiani, F.; Broll, V.; Evangelisti, E.; Ciurli, S. The Model Structure of the Copper-dependent Ammonia Monooxygenase. *J. Biol. Inorg. Chem.* **2020**, *25*, 995−1007.
(11) Ross, M. O.; MacMillan, F.; Wang, J.; Nisthal, A.; Lawton, T. J.; Olafson, B. D.; Mayo, S. L.; Rosenzweig, A. C.; Hoffman, B. M. Particulate Methane Monooxygenase Contains only Mononuclear Copper Centers. *Science* **2019**, *364*, 566−570.
(12) Park, Y.; Kim, Y.; Chang, S. Transition Metal-Catalyzed C−H Amination: Scope, Mechanism, and Applications. *Chem. Rev.* **2017**, *117*, 9247−9301.
(13) Clark, J. R.; Feng, K.; Sookezian, A.; White, M. C. Manganese-catalysed Benzylic C($sp^3$)−H Amination for Late-stage Functionalization. *Nat. Chem.* **2018**, *10*, 583−591.
(14) Ruiz-Castillo, P.; Buchwald, S. L. Applications of Palladium-Catalyzed C−N Cross-Coupling Reactions. *Chem. Rev.* **2016**, *116*, 12564−12649.
(15) Ouyang, K.; Hao, W.; Zhang, W.-X.; Xi, Z. Transition-Metal-Catalyzed Cleavage of C−N Single Bonds. *Chem. Rev.* **2015**, *115*, 12045−12090.
(16) Wang, Q.; Su, Y.; Li, L.; Huang, H. Transition-metal Catalysed C−N Bond Activation. *Chem. Soc. Rev.* **2016**, *45*, 1257−1272.
(17) Katritzky, A. R.; Marson, C. M. Pyrylium Mediated Transformations of Primary Amino Groups into Other Functional Groups. New Synthetic Methods (41). *Angew. Chem., Int. Ed.* **1984**, *23*, 420−429.
(18) Ni, S.; Li, C.-X.; Mao, Y.; Han, J.; Wang, Y.; Yan, H.; Pan, Y. Ni-catalyzed deaminative cross-electrophile coupling of Katritzky salts with halides via C−N bond activation. *Sci. Adv.* **2019**, *5*, No. eaaw9516.
(19) Zeng, X.; Yan, W.; Zacate, S. B.; Cai, A.; Wang, Y.; Yang, D.; Yang, K.; Liu, W. Copper-Catalyzed Deaminative Difluoromethylation. *Angew. Chem., Int. Ed.* **2020**, *59*, 16398−16403.
(20) Baker, K. M.; Baca, D. L.; Plunkett, S.; Daneker, M. E.; Watson, M. P. Engaging Alkenes and Alkynes in Deaminative Alkyl−Alkyl and Alkyl−Vinyl Cross-Couplings of Alkylpyridinium Salts. *Org. Lett.* **2019**, *21*, 9738−9741.
(21) Scharfbier, J.; Gross, B. M.; Oestreich, M. Stereospecific and Chemoselective Copper-Catalyzed Deaminative Silylation of Benzylic Ammonium Triflates. *Angew. Chem., Int. Ed.* **2020**, *59*, 1577−1580.
(22) Zhang, X.; Qi, D.; Jiao, C.; Liu, X.; Zhang, G. Nickel-catalyzed Deaminative Sonogashira Coupling of Alkylpyridinium Salts Enabled by NN2 Pincer Ligand. *Nat. Commun.* **2021**, *12*, 4904.
(23) Plunkett, S.; Basch, C. H.; Santana, S. O.; Watson, M. P. Harnessing Alkylpyridinium Salts as Electrophiles in Deaminative Alkyl−Alkyl Cross-Couplings. *J. Am. Chem. Soc.* **2019**, *141*, 2257−2262.
(24) Ashley, M. A.; Rovis, T. Photoredox-Catalyzed Deaminative Alkylation via C−N Bond Activation of Primary Amines. *J. Am. Chem. Soc.* **2020**, *142*, 18310−18316.
(25) Dorsheimer, J. R.; Ashley, M. A.; Rovis, T. Dual Nickel/Photoredox-Catalyzed Deaminative Cross-Coupling of Sterically Hindered Primary Amines. *J. Am. Chem. Soc.* **2021**, *143*, 19294−19299.
(26) Zhou, M.-G.; Zhang, W.-Z.; Tian, S.-K. Direct Enantiospecific Substitution of Primary a-aminoalkylferrocenes via Lewis Acid-catalyzed C−N Bond Cleavage. *Chem. Commun.* **2014**, *50*, 14531−14534.
(27) Kalutharage, N.; Yi, C. S. Deaminative and Decarboxylative Catalytic Alkylation of Amino Acids with Ketones. *Angew. Chem., Int. Ed.* **2013**, *52*, 13651−13655.
(28) Li, Y.; Handunneththige, S.; Xiong, J.; Guo, Y.; Talipov, M. R.; Wang, D. Opening the $Co^{III,IV}_2(\mu\text{-}O)_2$ Diamond Core by Lewis Bases Leads to Enhanced C-H Bond Cleaving Reactivity. *J. Am. Chem. Soc.* **2020**, *142*, 21670−21678.
(29) Li, Y.; Handunneththige, S.; Farquhar, E. R.; Guo, Y.; Talipov, M. R.; Li, F.; Wang, D. Highly Reactive $Co^{III,IV}_2(\mu\text{-}O)_2$ Diamond Core Complex that Cleaves C-H Bonds. *J. Am. Chem. Soc.* **2019**, *141*, 20127−20136.
(30) Cho, Y. I.; Joseph, D. M.; Rose, M. J. "Criss-Crossed" Dinucleating Behavior of an N4 Schiff Base Ligand: Formation of a $\mu$-OH,$\mu$-$O_2$ Dicobalt(III) Core via $O_2$ Activation. *Inorg. Chem.* **2013**, *52*, 13298−13300.
(31) Kotani, H.; Hong, D.; Satonaka, K.; Ishizuka, T.; Kojima, T. Mechanistic Insight into Dioxygen Evolution from Diastereomeric m-Peroxo Dinuclear Co(III) Complexes Based on Stoichiometric Electron-Transfer Oxidation. *Inorg. Chem.* **2019**, *58*, 3676−3682.
(32) Wang, H.-Y.; Mijangos, E.; Ott, S.; Thapper, A. Water Oxidation Catalyzed by a Dinuclear Cobalt−Polypyridine Complex. *Angew. Chem., Int. Ed.* **2014**, *53*, 14499−14502.
(33) Bezdek, M. J.; Guo, S.; Chirik, P. J. Coordination-induced Weakening of Ammonia, Water, and Hydrazine X−H Bonds in a Molybdenum Complex. *Science* **2016**, *354*, 730−733.
(34) Bhattacharya, P.; Heiden, Z. M.; Wiedner, E. S.; Raugei, S.; Piro, N. A.; Kassel, W. S.; Bullock, R. M.; Mock, M. T. Ammonia Oxidation by Abstraction of Three Hydrogen Atoms from a Mo−$NH_3$ Complex. *J. Am. Chem. Soc.* **2017**, *139*, 2916−2919.
(35) Anslyn, E. V.; Dougherty, D. A., Experiments Related to Thermodynamics and Kinetics. In *Modern Physical Organic Chemistry*; University Science: 2005; pp. 421−441.
(36) Large, T. A. G.; Mahadevan, V.; Keown, W.; Stack, T. D. P. Selective Oxidation of Exogenous Substrates by a bis-Cu(III) bis-oxide Complex: Mechanism and Scope. *Inorg. Chim. Acta* **2019**, *486*, 782−792.


https://doi.org/10.1021/jacs.2c13199
J. Am. Chem. Soc. 2023, 145, 2690−2697